Int J Adv Manuf Technol (2012) 61:569–584
DOI 10.1007/s00170-011-3737-0

ORIGINAL ARTICLE

A control algorithm for a vertical five-axis turning centre

Vladimir Kvrgic · Zoran Dimic · Vojkan Cvijanovic · Dragomir Ilic · Mirko Bucan

Received: 21 June 2011 / Accepted: 28 October 2011 / Published online: 27 November 2011

Abstract It is very useful to accomplish turning and five-axis milling, drilling and boring in only one setup, which is possible on five-axis turning centres. In this paper, we present a control algorithm for this machine with two translational and three rotational axes. The turning centre has a two rotary axis head with axes that do not intersect. This increases the possibility of machining and allows for certain types of machining without the machine taking the singular positions. The high angular speed of the table required for turning causes heating of the table-bearing support and base thermal deflection. If milling or drilling is done immediately after turning, the motion of the machine axis should be corrected to eliminate the error in machining that arises because of the deflection, a correction that has been done in this paper. The solution for the forward and inverse kinematics for this type of machine allows for programming the machine motion as if the machining were performed on a five-axis gantry milling machine. This has essentially facilitated machine programming.

Keywords Vertical five-axis turning centres · Control algorithm · Thermal errors

1 Introduction

Currently, the precision and productivity that users demand from the five-axis machining of complex workpiece surfaces is gradually increasing. To satisfy these requirements, different structures of five-axis machines were developed. The aim of this paper is focused on the development of a multifunctional vertical five-axis turning centre that allows for turning and five-axis milling and drilling and threading at the displaced worktable centre and at various angles. To provide the possibility for the machine to perform more types of machining in a single setup, time can be saved by relocating the workpiece from one machine to another. This significantly increases the machining productivity and accuracy.

At the present time, three configurations are common in five-axis milling centres. Starting from the workpiece and moving towards the tool tip [1, 2], where T means translational and R is the rotation axis, the machine denominations are given as follows: The cutting tool, a TTTRR type, is supported by a two-axis rotary head—one for head rotation and the other for tool tilting. This configuration is used in large gantry machine tools. The workpiece, an RRTTT type, is supported by a double rotation table, i.e. the worktable has two rotational axes. This configuration is commonly used in small compact machines. The workpiece, an RTTTR type, is supported by a rotary turning table, and the tool has one rotational degree of freedom (swivelling head).

With regard to the vertical lathes, the best five-axis milling and drilling performances on these machines are achieved by placing a rotary turning table on the *Y*-axis slider, which has an overall travel that is longer than the maximum diameter of turning [1]. Here, the worktable becomes the axis of auxiliary motion (C_y swivelling axis). For five-axis machining, the machine has turning, milling and drilling units, with the possibility of accepting a single-axis head with a B_t axis. In this way, the vertical lathe becomes a vertical five-axis gantry milling machine with *X*, *Y*, *Z*, B_t and C_y axes. This is an RTTTR machine type.

V. Kvrgic (✉) · Z. Dimic · V. Cvijanovic · D. Ilic · M. Bucan
Lola Institute,
Kneza Viseslava 70a,
11030 Belgrade, Serbia
e-mail: vladimir.kvrgic@li.rs

Using such a machine presents great possibilities. One drawback, however, is the complicated, long and heavy base of the *Y*-axis slider. In addition, these machines are very expensive. They also require a large workshop space.

Moreover, there are also lathes with the C_y axis and a small *Y*-axis (up to 200 mm), which are placed on the ram and carry an angular head along the B_t axis; therefore, such machine types are also of the RTTTR type. These machines cannot achieve five-axis milling across the entire worktable.

The present paper deals with the development of a vertical five-axis turning centre, where the worktable becomes the C_y axis. The swivelling of this axis, with a cutting tool motion along the *X*-axis according to the corresponding law, produces motion corresponding to the motion along the *Y*-axis. The turning, drilling and milling units can accept the replaceable two-axis angular head. In this way, a machine with two translational and three rotational axes can be obtained. This is an RTTRR machine type with C_y, *X*, *Z*, B_t and C_t axes. The working mechanism of this machine is illustrated in Fig. 1a.

Although during machining, different errors in the control algorithm, such as geometric errors [3–7], kinematics errors [1, 8], stiffness errors [1], thermal errors [9–12] and errors from the deflection of the cutting tools [1, 13, 14] influence the accuracy of the final parts, in this work, only the compensation of the shifting of the worktable axis caused by the machine base thermal deflection has been carried out. It was done because as a result of the parallelism of this axis with the C_t axis, the elimination of this error complicates the control algorithm by moving the C_y axis greatly. Specifically, if it is a matter of high-speed turning that lasts a long time, the worktable bearing and machine base temperature will significantly increase. This could cause thermal distortion. Although this deflection could be decreased by intensive cooling, it can exist during machining and influence the accuracy of the work.

Figure 2 shows the assembly of the single-column vertical lathe JVS 16 of the ILR factory. If we divide the machine structure in the *XZ* plane through the worktable bearing, we could see that the front part of the machine, which consists of the semicircular part of the machine base, is considerably smaller than the machine part behind the *XZ* plane, which consists of the rectangular part of the machine base, the column, the traverse with the ram cross-section and the ram, which can hold an angular head. The asymmetrical nature of the machine structure in relation to the *XZ* plane could, in the case of the worktable-bearing temperature significantly increases, cause the worktable rotational axis to shift by a few tenths of a millimetre in the imaginary *Y*-axis direction.

Although the machine base is designed to be thermally symmetrical relative to the imaginary *Y*-axis, a minimal thermal deflection along the *X*-axis can also happen. An undesirable thermal deflection of the machine base in the *X*-direction causes inaccuracy in turning. Thermal deflection along the *Y*-axis has practically no effect on the turning accuracy because it takes place along the tangent relative to the diameter of turning, which then changes negligibly. The worktable moving along the *X* and *Y*-axes has the impact on the milling and the drilling accuracy. Because of this, real-

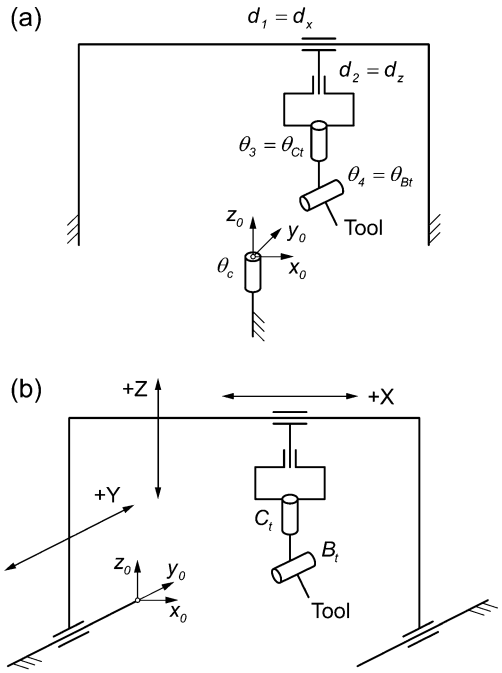

Fig. 1 **a** The inner coordinates of a five-axis turning centre with an RTTRR mechanism. **b** The tool coordinates of a TTTRR machine type, which are used for programming the RTTRR machine type

Fig. 2 The assembly of the single-column vertical lathe JVS 16 of the ILR factory

time measurements and a correction of the machine axes movement are required if milling or drilling is done immediately after turning. This is done by machine control algorithm suggested in this paper.

The forward and inverse kinematics for different kinds of five-axis milling machines have been presented and discussed in many papers, such as in [15] or [16]. Kinematic chain design and the utility of different kinds of five-axis machines are discussed in [17].

In this work, the forward and inverse kinematics have been solved for the vertical lathe with two translational and three rotational axes, which, for the five-axis milling, should enable the motion accomplished by three translational and two rotational axes. Consequently, the given control algorithm enables programming tool locations in milling or drilling as if it were machining on a five-axis gantry milling machine (TTTRR type), as shown in Fig. 1b. This has been done for a machine with an angular head, with axes that do not intersect, as shown in Fig. 3. The angular head increases the machining possibilities and helps to avoid some singular positions of the machine worktable. The control algorithm for the worktable axis, C_y, and the angular head axis, C_t, has been given, eliminating a number of their singular positions. Possible singular positions of these two parallel axes have been discussed. The proposed control algorithm fully eliminates the inaccuracy in machining caused by worktable displacements arising from thermal errors. In order to reduce the additional positioning of the table and the angular head during milling, the table swivelling angle θ_c has been expanded in the range of approximate ±360°. All of the above have additionally made solving the forward and inverse kinematics more complex. However, it has increased the machining possibilities and it has facilitated machine programming of five-axis turning centre.

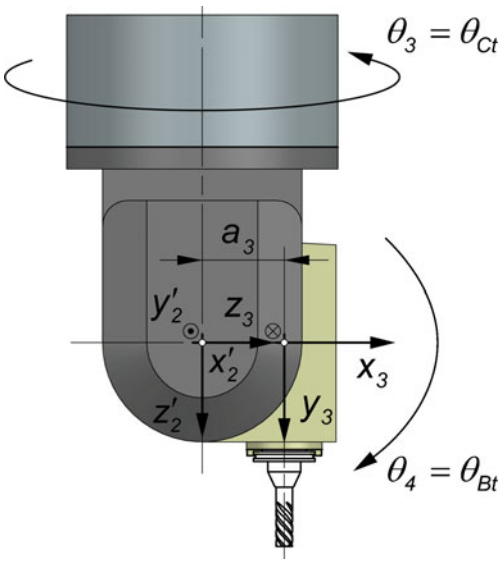

Fig. 3 Two-axis angular head with non-intersecting axes

2 Coordinate frames of machine components and matrices determining their relations

This section defines the coordinate frames for the components of a vertical five-axis turning centre (Fig. 4) and the matrices determining their relations. The machine components, their links and their coordinate frames are denoted using the Denavit–Hartenberg convention (D–H) [3, 18, 19]. The machine is viewed as a system with two entities performing a cooperative motion—one entity comprises a swivelling worktable with a workpiece, and the other is a serial mechanism with four links carrying the cutting tool. The machine base is denoted by 0, the serial components are denoted by 1 for the *X*-axis, 2 for the *Z*-axis, 3 for the C_t axis and 4 for the B_t axis, and the worktable axis (C_y) is denoted by 5. The first two serial links are translational and the other two are rotational; therefore, the corresponding axis variables are $d_1=d_x$, $d_2=d_z$, $\theta_3=\theta_{Ct}$ and $\theta_4=\theta_{Bt}$. The angle of the worktable rotation is denoted by $\theta_5=\theta_c$. This angle is the fifth axis variable. The adopted convention specifies that the angle θ_3 is positive when the component's 3 rotation is in the negative mathematical direction, and the angles θ_4 and θ_c are positive when the component's 4 rotation and the rotating table are in the positive mathematical direction. The thermal deflection along the *X* and *Y*-axes are denoted by δ_{xc} and δ_{yc} (Fig. 4). D–H parameters of the machine components are given in Table 1.

In this paper, we will adopt the RPY orientation angles of the tool. The angular head (Fig. 3) has angles B_t and C_t. Figure 5a shows the case with $\theta_3=\theta_c$ and $\theta_4=90°$. Here, $C_t=0°$ and $B_t=90°$. Figure 5b shows the case with $\theta_3=\theta_c-180°$ and $\theta_4=-90°$. Here, $C_t=180°$ and $B_t=-90°$. In both cases, the tool z_t axis is perpendicular to the worktable y_c axis.

The homogenous matrix that transforms the coordinates of a point from frame $x_n y_n z_n$ to frame $x_m y_m z_m$ is denoted by ${}^n\mathbf{T}_m$. This matrix, which describes the relation between one link and the next, is called $\mathbf{A}_i=\mathbf{A}(i\text{-}1,i)$ [19]. The following homogenous matrices for the relation between the coordinate frames of the machine links are defined to derive the kinematic equations for the machine:

$$\begin{aligned}\mathbf{A}_1 &= \mathbf{A}(0,1)\\ &= \mathbf{Trans}(z_0,d_{zc})\mathbf{Rot}(z_0,\theta_{1a})\mathbf{Rot}(x'_0,\alpha_1)\mathbf{Trans}(z''_0,d_x)\mathbf{Rot}(x''_0,\alpha'_1)\end{aligned}$$

$$\mathbf{A}_2 = \mathbf{A}(1,2) = \mathbf{Trans}(z_1,d_z)$$

$$\begin{aligned}\mathbf{A}_3 &= \mathbf{A}(2,3)\\ &= \mathbf{Rot}(z_2,\theta_{3a})\mathbf{Rot}(z''_2,\theta_3)\mathbf{Trans}(x''_2,a_3)\mathbf{Rot}(x''_2,\alpha_3)\end{aligned}$$

$$\mathbf{A}_4 = \mathbf{A}(3,4) = \mathbf{Rot}(z_3,\theta_4)\ \mathbf{Rot}(x'_3,\alpha_4)$$

$$\mathbf{A}_c = \mathbf{A}(0,c) = \mathbf{Trans}(x_0,\delta_{xc})\mathbf{Trans}(y_0,\delta_{yc})\mathbf{Rot}(z_0,\theta_c)$$

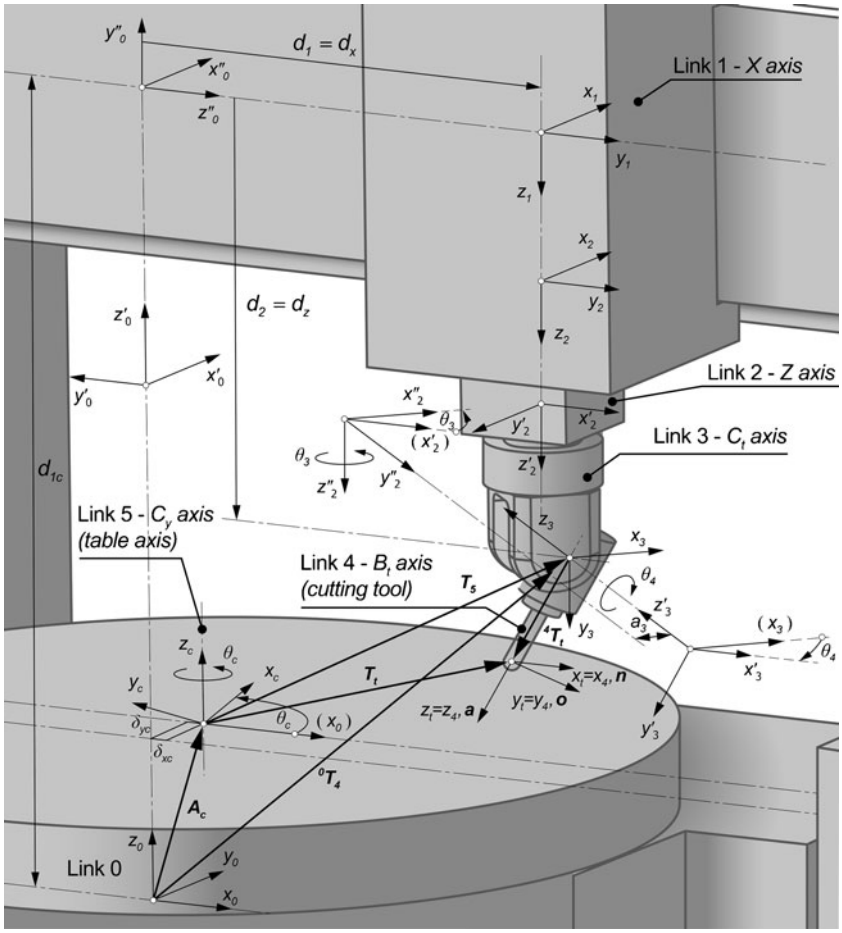

Fig. 4 Coordinate frames of the vertical five-axis turning centre components

By using the convenient shorthand notation, $\sin(\theta_\varphi)=s_\varphi$ and $\cos(\theta_\varphi)=c_\varphi$ and the transformation matrices defined above are written as follows:

$$\mathbf{A}_1 = \begin{bmatrix} 0 & 1 & 0 & d_x \\ 1 & 0 & 0 & 0 \\ 0 & 0 & -1 & d_{zc} \\ 0 & 0 & 0 & 1 \end{bmatrix} \quad (1)$$

$$\mathbf{A}_2 = \begin{bmatrix} 1 & 0 & 0 & 0 \\ 0 & 1 & 0 & 0 \\ 0 & 0 & 1 & d_z \\ 0 & 0 & 0 & 1 \end{bmatrix} \quad (2)$$

$$\mathbf{A}_3 = \begin{bmatrix} s_3 & 0 & c_3 & s_3 a_3 \\ c_3 & 0 & -s_3 & c_3 a_3 \\ 0 & 1 & 0 & 0 \\ 0 & 0 & 0 & 1 \end{bmatrix} \quad (3)$$

$$\mathbf{A}_4 = \begin{bmatrix} c_4 & 0 & -s_4 & 0 \\ s_4 & 0 & c_4 & 0 \\ 0 & -1 & 0 & 0 \\ 0 & 0 & 0 & 1 \end{bmatrix} \quad (4)$$

$$\mathbf{A}_c = \begin{bmatrix} c_c & -s_c & 0 & \delta_{xc} \\ s_c & c_c & 0 & \delta_{yc} \\ 0 & 0 & 1 & 0 \\ 0 & 0 & 0 & 1 \end{bmatrix} \quad (5)$$

Table 1 D–H parameters of vertical five-axis turning centre components

Link	Variable	a [mm]	a_y [mm]	d [mm]	α [°]	θ [°]
1-X	$d_1=d_x$	0	0	$d_{1c}=d_{zc}$	$\alpha_1=90$, $\alpha'_1=90$	$\theta_{1a}=90$
2-Z	$d_2=d_z$	0	0	0	0	0
3-C_t	$(-)\theta_3=\theta_{Ct}$	a_3	0	0	$\alpha_3=90$	$\theta_{3a}=90$
4-B_t	$\theta_4=\theta_{Bt}$	0	0	0	$\alpha_4=-90$	0
5-C_y	$\theta_5=\theta_c$	δ_{xc}	δ_{yc}	0	0	0

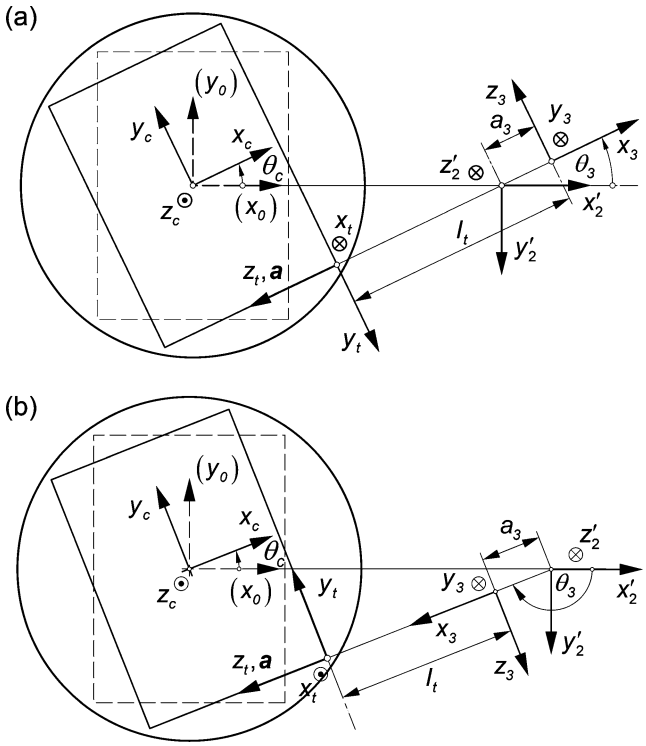

Fig. 5 Coordinate frames of the table and the tool when **a** $\theta_3=\theta_c$, $\theta_4=90°$, $C_t=0°$ and $B_t=90°$; **b**: $\theta_3=\theta_c-180°$, $\theta_4=-90°$, $C_t=180°$ and $B_t=-90°$

3 Programming of the five-axis vertical turning centre

First of all, the programming of the five-axis milling, drilling and boring operations on the vertical turning centre are performed by a CAM system or manually by G code [1, 20] in the machine base coordinates $x_0y_0z_0$ (Fig. 4) as if it were machining on a five-axis gantry milling machine, where the workpiece is fixed (TTTRR machine type), as shown in Fig. 1b. This is possible because the solutions for the forward and inverse kinematics proposed in this work allow for the tool locations relative to the swivelling workpiece to be identical to the tool locations relative to the immobile workpiece. This will essentially facilitate easy machine programming. Using G code, the tool direction is given in the *X*, *Y* and *Z* coordinates, and the tool orientation is given in Euler or RPY angles or by the tool direction vector, which points from the tooltip towards the tool holder. If we define the approach vector as $\mathbf{a}=a_{x5}\mathbf{i}+a_{y5}\mathbf{j}+a_{z5}\mathbf{k}$, which lies in the z_t direction from which the tool approaches the workpiece (Fig. 4), the tool direction vector components will be $-a_{x5}$, $-a_{y5}$ and $-a_{z5}$. Here, **i**, **j** and **k** are unit vectors along the x_0, y_0 and z_0 machine base coordinates. Using a CAM system, the output is the toolpath, which is defined by the cutter locations, *X*, *Y*, *Z*, $-a_{x5}$, $-a_{y5}$ and $-a_{z5}$, which define the tool positions and the tool direction vectors with respect to the workpiece coordinate system, given in the CL data file [15, 16, 18]. The toolpath between two CL points is a straight line relative to the workpiece.

The following step after the toolpath generation is post-processing, where the programme is translated to a specified machine and control unit [15, 20]. The post-processor converts the CL motion commands from the CL data file to the motion commands of the NC programme (in G code). The post-processed G codes are input format to the next step.

Finally, the toolpath is converted into a sequence of consecutive positions of machine axes that will produce the desired tool locations (inverse kinematics). This transmission can be carried out using three different methods.

In the first method, the post-process or carries out the inverse kinematics in full. In each interpolation period, the interpolator interpolates all of the machine axes [18]. Because of the rotary axes, the toolpath between the two blocks in the NC programme will be non-linear relative to the workpiece, reducing the accuracy of the toolpath. Linearisation of the toolpath can be performed in the post-processor by interpolating the new CL data point along the ideal toolpath and thereby adding new blocks to the NC programme.

In the second method, the NC unit carries out the interpolation of the toolpath in real time and then, in each interpolation period, calculates the inverse kinematics. In this way, the NC unit manages the speed and the location of the tool during machining. This solution improves the quality of the toolpath. The controller used in this work calculates the path interpolation and the inverse kinematics in real time [21].

The third method is a hybrid method: the post-processor carries out the calculation of the rotation axes, and the control unit carries out the calculation of the translational axes. An interpolation of all the machine axes, and not of the toolpath, is performed here.

4 Forward kinematics

Forward kinematics are used to calculate the tool position and orientation, *X*, *Y*, Z, B_t and C_t, with respect to the machine axis variables, d_1, d_2, θ_3, θ_4 and θ_c, and the thermal deflection, δ_{xc} and δ_{yc}. It is obvious from Fig. 4 that the component 4 position and orientation relative to the machine base is given by the equation ${}^0\mathbf{T}_4=\mathbf{A}_1\mathbf{A}_2\mathbf{A}_3\mathbf{A}_4$ and relative to the rotating workpiece by the equation:

$$\mathbf{T}_5=\mathbf{A}_c^{-1}\mathbf{A}_1\,\mathbf{A}_2\,\mathbf{A}_3\mathbf{A}_4 = \begin{bmatrix} c_cc_{34}+s_cs_3c_4 & c_cs_3-s_cc_3 & -c_cc_3s_4-s_cs_{34} & X_5 \\ -s_cc_{34}+c_cs_3c_4 & -s_cs_3-c_cc_3 & s_cc_3s_4-c_cs_{34} & Y_5 \\ -s_4 & 0 & -c_4 & Z_5 \\ 0 & 0 & 0 & 1 \end{bmatrix} \quad (6)$$

where $X_5 = c_c(d_x + c_3a_3 - \delta_{xc}) + s_c(s_3a_3 - \delta_{yc})$, and $Y_5 = -s_c(d_x + c_3a_3 - \delta_{xc}) + c_c(s_3a_3 - \delta_{yc})$, $Z_5 = d_{zc} - d_z$.

The tool location relative to the rotating workpiece is determined by the matrix:

$$\mathbf{T}_t = \mathbf{T}_5{}^4\mathbf{T}_t = \mathbf{T}_5 \begin{bmatrix} 1 & 0 & 0 & -r_t \\ 0 & 1 & 0 & 0 \\ 0 & 0 & 1 & l_t \\ 0 & 0 & 0 & 1 \end{bmatrix}$$

$$= \begin{bmatrix} c_c c_{34} + s_c s_3 c_4 & c_c s_3 - s_c c_3 & -c_c c_3 s_4 - s_c s_{34} & X \\ -s_c c_{34} + c_c s_3 c_4 & -s_c s_3 - c_c c_3 & s_c c_3 s_4 - c_c s_{34} & Y \\ -s_4 & 0 & -c_4 & Z \\ 0 & 0 & 0 & 1 \end{bmatrix}$$

$$= \begin{bmatrix} n_{x5} & o_{x5} & a_{x5} & X \\ n_{y5} & o_{y5} & a_{y5} & Y \\ n_{z5} & o_{z5} & a_{z5} & Z \\ 0 & 0 & 0 & 1 \end{bmatrix} \tag{7}$$

where: $X = X_5 - (c_c c_{34} + s_c s_3 c_4)r_t - (c_c c_3 s_4 + s_c s_{34})l_t$, and $Y = Y_5 + (s_c c_{34} - c_c s_3 c_4)r_t + (s_c c_3 s_4 - c_c s_{34})l_t$ and $Z = Z_5 + s_4 r_t - c_4 l_t$.

Here, ${}^4\mathbf{T}_t$ is the tool position matrix relative to the component 4, l_t is the length and r_t is the radius of the tool (Fig. 4). In the initial position, shown in Fig. 6, and for $\delta_{xc}=\delta_{yc}=0$, the location is $\theta_c=\theta_3=\theta_4=C_t=B_t=0^o$ and

$$\mathbf{T}_t = \begin{bmatrix} 1 & 0 & 0 & d_x - r_t \\ 0 & -1 & 0 & 0 \\ 0 & 0 & -1 & d_{zc} - d_z - l_t \\ 0 & 0 & 0 & 1 \end{bmatrix} \tag{8}$$

Now, using the tool orientation matrix, [**n o a**], and Eq. 7, the tool orientation angles can be determined.

4.1 Calculations of the RPY tool orientation angles

The following section describes the analysis and a discussion of the solutions used to calculate the RPY tool orientation angles [19]. By using these angels, the orientation vector results from turning a vector in the z direction firstly with $-180° \le C_t \le 180°$ around the z-axis

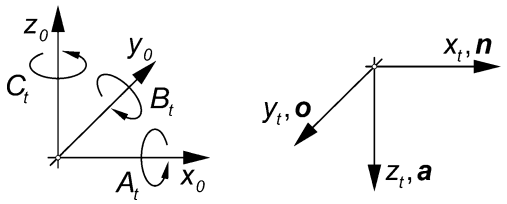

Fig. 6 The coordinate frames of the machine base and the cutting tool in an initial position

(roll), then with $-90° \le B_t \le 90°$ around the new y-axis (pitch) and lastly with $-180° \le A_t \le 180°$ (here is $A_t=180°$) around the new x-axis (yaw), ORIZYX(C_t,B_t,A_t). RPY angels could be defined with three rotations around the station axes. Here, the orientation vector results from turning a vector in the z-direction firstly with A_t around the x_0 axis, then with B_t around the station y_0 axis and lastly with C_t around the station z_0 axis, ORIRS(A_t,B_t,C_t). The tool orientation matrix for the RPY angles and for the case when $A_t=180°$ reads:

ORIZYX(C_t,B_t,A_t)=**R**ot(z,C_t) **R**ot(y,B_t) **R**ot(x,A_t), i.e.,

$$\begin{bmatrix} n_{x5} & o_{x5} & a_{x5} \\ n_{y5} & o_{y5} & a_{y5} \\ n_{z5} & o_{z5} & a_{z5} \end{bmatrix} = \begin{bmatrix} c_{C_t} c_{B_t} & s_{C_t} & -c_{C_t} s_{B_t} \\ s_{C_t} c_{B_t} & -c_{C_t} & -s_{C_t} s_{B_t} \\ -s_{B_t} & 0 & -c_{B_t} \end{bmatrix} \tag{9}$$

From here, it is obtained that **R**ot(z,C_t)$^{-1}$ [**n o a**]=**R**ot(y,B_t) **R**ot(x,A_t), i.e.

$$\begin{bmatrix} c_{C_t} n_{x5} + s_{C_t} n_{y5} & c_{C_t} o_{x5} + s_{C_t} o_{y5} & c_{C_t} a_{x5} + s_{C_t} a_{y5} \\ -s_{C_t} n_{x5} + c_{C_t} n_{y5} & -s_{C_t} o_{x5} + c_{C_t} o_{y5} & -s_{C_t} a_{x5} + c_{C_t} a_{y5} \\ n_{z5} & o_{z5} & a_{z5} \end{bmatrix} = \begin{bmatrix} c_{B_t} & 0 & -s_{B_t} \\ 0 & -1 & 0 \\ -s_{B_t} & 0 & -c_{B_t} \end{bmatrix} \tag{10}$$

and [**n o a**] **R**ot(x,A_t)$^{-1}$ **R**ot(y,B_t)$^{-1}$=**R**ot(z,C_t), i.e.,

$$\begin{bmatrix} c_{B_t} n_{x5} - s_{B_t} a_{x5} & -o_{x5} & -s_{B_t} n_{x5} - c_{B_t} a_{x5} \\ c_{B_t} n_{y5} - s_{B_t} a_{y5} & -o_{y5} & -s_{B_t} n_{y5} - c_{B_t} a_{y5} \\ c_{B_t} n_{z5} - s_{B_t} a_{z5} & -o_{z5} & -s_{B_t} n_{z5} - c_{B_t} a_{z5} \end{bmatrix} = \begin{bmatrix} c_{C_t} & -s_{C_t} & 0 \\ s_{C_t} & c_{C_t} & 0 \\ 0 & 0 & 1 \end{bmatrix} \tag{11}$$

Using the matrix Eqs. 9, 10 and 11, it is possible to determine angles B_t and C_t in a few different ways. Some solutions differ by 180°. However, in some cases, when the argument of the function, *a*tan2, reads 0,0, inaccurate results are obtained. These solutions will be analysed as follows: By employing known values for these angles, we will, using Eq. 9, yield the matrix [**n o a**]. Afterwards, using this matrix, the orientation angles will be calculated. Only the solutions in which each tool orientation yields solutions equal to the starting tool orientation angles will be adopted.

4.1.1 Calculations of the angle B_t

Terms (3,1) and (3,3) of matrix Eqs. 9 and 10 yield

$$B_t = \text{atan2}(-n_{z5}, -a_{z5}) \tag{12}$$

This solution is independent of the angle C_t while components n_{z5} and a_{z5} (Fig. 7) of the argument of the function atan2 are not simultaneously equal to zero in any position of the tool. Consequently, this solution gives an accurate result in any tool position.

If the calculations for the angle B_t are done after those for the angle C_t, then other equations can also be used. Using terms (1,3) and (3,3) or (1,3) and (1,1) or (3,1) and (1,1), respectively, of Eq. 10, the Eqs. 13, 14 and 15 can be obtained. Similar to Eq. 12, Eqs. 13, 14 and 15 always yield accurate results.

$$B_t = \text{atan2}(-c_{Ct}a_{x5} - s_{Ct}a_{y5}, -a_{z5}) \tag{13}$$

$$B_t = \text{atan2}(-c_{Ct}a_{x5} - s_{Ct}a_{y5},\ c_{Ct}n_{x5} + s_{Ct}n_{y5}) \tag{14}$$

$$B_t = \text{atan2}(-n_{z5},\ c_{Ct}n_{x5} + s_{Ct}n_{y5}) \tag{15}$$

Term (1,3) of Eq. 11 (Fig. 7) yields the solutions:

$$B_t = \text{atan2}(a_{x5}, -n_{x5}) \tag{16}$$

and

$$B_t = \text{atan2}(-a_{x5}, n_{x5}) \tag{17}$$

The values for these two solutions differ by 180°. If $C_t \in(90°,180°)$ or $C_t \in(-90°,-180°)$, an accurate result is obtained by Eq. 16, and if $C_t \in(-90°,90°)$, an accurate result is obtained by Eq. 17. However, for the values of C_t= 90° and C_t=−90°, components n_{x5} and a_{x5} are always equal to zero. Therefore, these two equations are inapplicable in these cases.

The term (2,3) of Eq. 11 gives the solutions:

$$B_t = \text{atan2}(a_{y5}, -n_{y5}) \tag{18}$$

and

$$B_t = \text{atan2}(-a_{y5}, n_{y5}) \tag{19}$$

The values for these solutions also differ by 180°. If $C_t \in(0°,180°)$, an accurate result is obtained by Eq. 19, and if $C_t \in(0°,-180°)$, an accurate result is obtained by Eq. 18. However, for the values of C_t=0° and C_t=180°, components n_{y5} and a_{y5} are always equal to zero, and the two equations in these two cases are inapplicable.

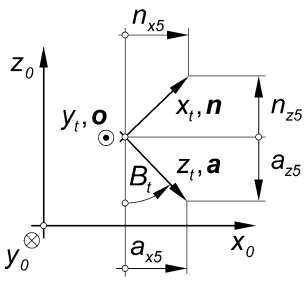

Fig. 7 Tool orientation vector components

4.1.2 Calculations of the angle C_t

Terms (1,2) and (2,2) of Eq. 11 give:

$$C_t = \text{atan2}(o_{x5}, -o_{y5}) \tag{20}$$

Components o_{x5} and o_{y5} of the function atan2 are independent of angle B_t. They always lie in the x_0y_0 plane, which means that they are never simultaneously equal to zero (o_{z5}=0). Therefore, Eq. 20 can be used to calculate angle C_t.

When the value of angle B_t is known, angle C_t can be calculated using Eqs. 21, 22 and 23, obtained by terms (2,1) and (1,1), or (1,2) and (1,1), or (2,2) and (1,1) of Eq. 11, respectively.

$$C_t = \text{atan2}(c_{Bt}n_{y5} - s_{Bt}a_{y5},\ c_{Bt}n_{x5} - s_{Bt}a_{x5}) \tag{21}$$

$$C_t = \text{atan2}(o_{x5},\ c_{Bt}n_{x5} - s_{Bt}a_{x5}) \tag{22}$$

$$C_t = \text{atan2}(c_{Bt}n_{y5} - s_{Bt}a_{y5}, -o_{y5}) \tag{23}$$

Like Eq. 20, Eqs. 21, 22 and 23 always yield accurate results.

Term (2,3) of Eq. 10 gives the solutions:

$$C_t = \text{atan2}(a_{y5}, a_{x5}) \tag{24}$$

and

$$C_t = \text{atan2}(-a_{y5}, -a_{x5}) \tag{25}$$

The values of these two solutions differ by 180°. If $B_t \in(-90°,0°)$, an accurate result yields Eq. 24, and if $B_t \in(90°,0°)$, an accurate result yields Eq. 25. However, for B_t=0°, components a_{x5} and a_{y5} are always equal to 0, and these two equations are, in this case, inapplicable. For B_t=0°, we can adopt C_t=0°.

Term (1,2) of Eq. 10 gives two solutions:

$$C_t = \text{atan2}(n_{y5}, n_{x5}) \tag{26}$$

and

$$C_t = \text{atan2}(-n_{y5}, -n_{x5}) \tag{27}$$

If $B_t \in(-90°,90°)$, Eq. 26 yields an accurate result, and Eq. 27 yields a result differing by ±180°. However, for B_t=±90°, components n_{x5} and n_{y5} are always equal to 0, and these two equations are, in this case, inapplicable.

5 Inverse kinematics

Inverse kinematics are used to determine the axes variables d_1, d_2, θ_3, θ_4 and θ_c by using the desired cutter location, X, Y, Z, $-a_{x5}$, $-a_{y5}$ and $-a_{z5}$, given in the CL data file, or using X, Y, Z, C_t and B_t given in G code. The control unit, during machining in each interpolation period, determines the tool locations and corresponding positions of the machine axes.

This section discusses some of the possible singular positions of the machine as well. The given control algorithm eliminates some of the singular positions of the rotating table and the head axis, C_t.

By virtue of the tool position and the orientation relative to the rotating table and given by the matrix, $\mathbf{T}_t$, Eq. 7, we will determine the machine components positions. The position of component 4, with respect to the rotating table, is defined by the equation:

$$\mathbf{T}_5 = \mathbf{T}_t \, {}^4\mathbf{T}_t^{-1} \tag{28}$$

Now, using the tool orientation matrix for the RPY angles and for A_t=180°, Eq. 9, the preceding equation reads:

$$\mathbf{T}_5 = \begin{bmatrix} c_{C_t}c_{B_t} & s_{C_t} & -c_{C_t}s_{B_t} & c_{C_t}c_{B_t}r_t + c_{C_t}s_{B_t}l_t + X \\ s_{C_t}c_{B_t} & -c_{C_t} & -s_{C_t}s_{B_t} & s_{C_t}c_{B_t}r_t + s_{C_t}s_{B_t}l_t + Y \\ -s_{B_t} & 0 & -c_{B_t} & -s_{B_t}r_t + c_{B_t}l_t + Z \\ 0 & 0 & 0 & 1 \end{bmatrix}$$

$$= \begin{bmatrix} n_{x5} & o_{x5} & a_{x5} & X_5 \\ n_{y5} & o_{y5} & a_{y5} & Y_5 \\ n_{z5} & o_{z5} & a_{z5} & Z_5 \\ 0 & 0 & 0 & 1 \end{bmatrix} \tag{29}$$

It is clear that $X_5 = n_{x5}r_t - a_{x5}l_t + X$, $Y_5 = n_{y5}r_t - a_{y5}l_t + Y$, $Z_5 = n_{z5}r_t - a_{z5}l_t + Z$.

If we programme the machining using G code, we could, using parameters X, Y, Z, C_t and B_t, calculate the matrix, $\mathbf{T}_5$. If we programme the machining by a CAM system, we could first calculate C_t and B_t by Eqs. 25 or 24 and 13 and then calculate the matrix, $\mathbf{T}_5$.

By multiplying both sides of Eq. 6 by matrix $\mathbf{A}_c$ on the left side, we obtain:

$$\mathbf{A}_c\mathbf{T}_5 = {}^0\mathbf{T}_4 = \mathbf{A}_1\mathbf{A}_2\mathbf{A}_3\mathbf{A}_4, \text{ i.e.,}$$

$$\begin{bmatrix} c_c n_{x5} - s_c n_{y5} & c_c o_{x5} - s_c o_{y5} & c_c a_{x5} - s_c a_{y5} & c_c X_5 - s_c Y_5 + \delta_{xc} \\ s_c n_{x5} + c_c n_{y5} & s_c o_{x5} + c_c o_{y5} & s_c a_{x5} + c_c a_{y5} & s_c X_5 + c_c Y_5 + \delta_{yc} \\ n_{z5} & o_{z5} & a_{z5} & Z_5 \\ 0 & 0 & 0 & 1 \end{bmatrix} =$$

$$= \begin{bmatrix} c_{34} & s_3 & -c_3 s_4 & d_x + c_3 a_3 \\ s_3 c_4 & -c_3 & -s_{34} & s_3 a_3 \\ -s_4 & 0 & -c_4 & d_{zc} - d_z \\ 0 & 0 & 0 & 1 \end{bmatrix} \tag{30}$$

In Eq. 30, we calculate the terms of matrix $\mathbf{T}_5$ by Eq. 29. Multiplying Eq. 30 consecutively by ${\mathbf{A}_1}^{-1}$, then by ${\mathbf{A}_2}^{-1}$ and lastly by ${\mathbf{A}_3}^{-1}$ on the left side, we obtain: ${\mathbf{A}_3}^{-1}{\mathbf{A}_2}^{-1}{\mathbf{A}_1}^{-1}\mathbf{A}_c\,\mathbf{T}_5 = {}^3\mathbf{T}_4 = \mathbf{A}_4$

$$\text{i.e.} \begin{bmatrix} .... & .... & s_3(s_c a_{x5} + c_c a_{y5}) + c_3(c_c a_{x5} - s_c a_{y5}) & .... \\ .... & .... & -a_{z5} & .... \\ .... & .... & c_3(s_c a_{x5} + c_c a_{y5}) - s_3(c_c a_{x5} - s_c a_{y5}) & .... \\ 0 & 0 & 0 & 1 \end{bmatrix}$$

$$= \begin{bmatrix} c_4 & 0 & -s_4 & 0 \\ s_4 & 0 & c_4 & 0 \\ 0 & -1 & 0 & 0 \\ 0 & 0 & 0 & 1 \end{bmatrix} \tag{31}$$

5.1 Calculations of the table rotation angle θ_c

Term (2,4) of Eq. 30 reads:

$$s_c X_5 + c_c Y_5 + \delta_{yc} = s_3 a_3 \tag{32}$$

Term (1,2) of Eq. 30 yields:

$$s_3 = c_c o_{x5} - s_c o_{y5} \tag{33}$$

Terms (2,3) and (3,1) of Eq. 30 yield:

$$s_3 = (s_c a_{x5} + c_c a_{y5})/n_{z5} \tag{34}$$

Terms (2,1) and (3,3) of Eq. 30 yield:

$$s_3 = (-s_c n_{x5} - c_c n_{y5})/a_{z5} \tag{35}$$

It is possible to calculate s_3 only by the help of the components of vector $\mathbf{a}$, obtained from the CL data file; however, for this case, we need to have information on the sign of the angle, θ_4. Namely, for $\theta_4 \neq 0°$, terms (2,3) and (3,3) of Eq. 30 yield:

$$s_3 = (-s_c a_{x5} - c_c a_{y5}) \Big/ (\text{sign}(\theta_4)\sqrt{1 - a_{z5}^2}) \tag{36}$$

and for θ_4=0° the terms yield: s_3=0.

Now, Eq. 32 can be written in the following form:

$$\frac{\tan(\theta_c)}{\sqrt{1+\tan^2(\theta_c)}}\,p_x + \frac{p_y}{\sqrt{1+\tan^2(\theta_c)}} = -\delta_{yc} \tag{37}$$

Eqs. 33 and 37 yield:

$$p_x = X_5 + o_{y5}\,a_3 \quad \text{and} \quad p_y = Y_5 - o_{x5}\,a_3 \tag{38}$$

Eqs. 34 and 37 yield:

$$p_x = X_5 - a_{x5}\,a_3/n_{z5} \quad \text{and} \quad p_y = Y_5 - a_{y5}\,a_3/n_{z5} \tag{39}$$

Eqs. 35 and 37 yield:

$$p_x = X_5 + n_{x5}\, a_3/a_{z5} \quad \text{and} \quad p_y = Y_5 + n_{y5}\, a_3/a_{z5} \tag{40}$$

Eqs. 36 and 37 yield:

$$p_x = X_5 + a_{x5}\, a_3 \Big/ (\text{sign}(\theta_4)\, \sqrt{1 - a_{z5}^2}) \text{ and}$$
$$p_y = Y_5 + a_{y5}\, a_3 \Big/ (\text{sign}(\theta_4)\, \sqrt{1 - a_{z5}^2}) \text{ for } \theta_4 \neq 0° \tag{41}$$

and P_x=X_5 and P_y=Y_5 for θ_4=0°.

Eq. 37 can be written in the form: $p_x \tan(\theta_c) + p_y = -\delta_{yc}\sqrt{1+\tan^2(\theta_c)}$ and $p_x^2\tan^2(\theta_c) + p_y^2 + 2p_xp_y\tan(\theta_c) = \delta_{yc}^2(1+\tan^2(\theta_c))$ i.e. $(p_x^2 - \delta_{yc}^2)\tan^2(\theta_c) + 2p_xp_y\tan(\theta_c) + p_y^2 - \delta_{yc}^2 = 0$. The solution for the preceding equation is $\theta_c = \arctan((-p_xp_y \pm \sqrt{p_x^2p_y^2 - (p_x^2 - \delta_{yc}^2)(p_y^2 - \delta_{yc}^2)})/(p_x^2 - \delta_{yc}^2)$.

As the table swivelling angle decreases with the table moving in the direction of the y_0 axis, because of thermal deflections (δ_{yc} >0), the sign − will be adopted in the preceding equation such that:

$$\theta_{c90} = \text{atan2}(-p_xp_y - \delta_{yc}\sqrt{p_x^2 + p_y^2 - \delta_{yc}^2},\ p_x^2 - \delta_{yc}^2) \tag{42}$$

The table swivelling angle θ_c in Eq. 42 is denoted by θ_{c90} because this equation always gives angle θ_c in the range [−90°,90°] except when $p_x^2 < \delta_{yc}^2$, which is a special case.

5.1.1 Algorithm for calculation of the table rotation angle θ_c

The X-axis feed will be limited so that the cutting tool moves from the table centre to the maximum positive value. To achieve this, and also taking into consideration that the value of X_5 can be negative, the table swivelling angle θ_c should be in the minimum range of [−180°,180°]. To reduce the additional positioning of the table and the angular head during milling, the table swivelling angle θ_c will be adopted in the range of [−360°+θ_{c90}, 360°+θ_{c90}]. Hence, it is necessary to extend the range of angle θ_c, which is obtained by Eq. 42, from [−90°,90°] to [−360°+θ_{c90}, 360°+θ_{c90}]. To achieve this, but also to avoid the uncontrolled worktable swivelling in singular positions by approximately ±180° or ±360°, this paper proposes a novel algorithm for calculating angle θ_c. It consists of three steps, presented below. These steps are shown in Fig. 8.

Step 1 Step 1 involves the calculations of angle θ_c for the case without a thermal deflection of the machine base. The range of angle θ_c obtained here is [−180°,180°]. For δ_{yc}=0, Eq. 42 reads:

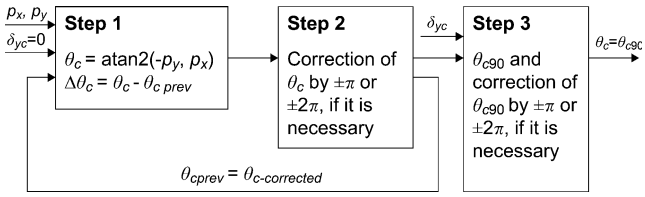

Fig. 8 The graph of the algorithm for calculation of the table rotation angle θ_c

$$\theta_c = \text{atan2}(-p_y,\ p_x) \tag{43}$$

Let angle θ_c be denoted by θ_{cprev} for the previous interpolation period. The angle θ_c increment for the next interpolation period will be:

$$\Delta\theta_c = \theta_c - \theta_{cprev} \tag{44}$$

Step 2 In step 2, we check if the value of angle θ_c, calculated in step 1 for a single interpolation period, changes by approximately $\Delta\theta_c$=±180° or $\Delta\theta_c$=±360°. The procedure, presented below, makes this changing impossible and, if necessary, extends the range of the angle θ_c from [−180°,180°] to [−360°,360°].

If $\theta_{cprev}\in[-\pi,\pi]$, then {
If $\Delta\theta_c > 3\pi/2$, then $\theta_c = \theta_c - 2\pi$;
If $\Delta\theta_c \in[\pi/2,3\pi/2]$, then $\theta_c = \theta_c - \pi$;
If $\Delta\theta_c \in [-\pi/2, -3\pi/2]$, then $\theta_c = \theta_c + \pi$;
And if $\Delta\theta_c, < -3\pi/2$, then$\theta_c = \theta_c + 2\pi$;}
Else {
If $\theta_c > 0$, then {
If $\theta_{cprev} \in [-\pi, -2\pi)$, then {$\theta_c = \theta_c - \pi$;
If$\Delta\theta_c > 3\pi/2$, then$\theta_c = \theta_c - \pi$;}
And if $\theta_{cprev} \in (\pi, 2\pi)$, then {
If $\Delta\theta_c \in [-\pi/2, -3\pi/2]$, then $\theta_c = \theta_c + \pi$;
And if$\Delta\theta_c, < -3\pi/2$, then $\theta_c = \theta_c + 2\pi$;}}
Else ($\theta_c \leq 0$) {
If $\theta_{cprev} \in (-\pi, -2\pi]$, then {
If $\Delta\theta_c \in [\pi/2, 3\pi/2]$, then$\theta_c = \theta_c - \pi$;
And if $\Delta\theta_c > 3\pi/2$, then $\theta_c = \theta_c - 2\pi$;}
And if $\theta_{cprev} \in (\pi, 2\pi)$, then {$\theta_c = \theta_c + \pi$;
If $\Delta\theta_c < -3\pi/2$, then $\theta_c = \theta_c + \pi$;}}}

For calculation of angle θ_c in the next interpolation period, the value will be assigned as θ_{cprev}=θ_c.

Step 3 In step 3, angle θ_c is determined for the case of $\delta_{yc}\neq$ 0. First, by using Eq. 42, the value of angle θ_{c90} is calculated. Using this and the value of angle θ_c obtained in step 2, the range of angle θ_c is extended from [−90°,90°] to [−360°+θ_{c90},360°+θ_{c90}].

The difference between angle θ_{c90}, obtained by Eq. 42, and angle θ_c as calculated in step 2 will be denoted by:

$$\Delta\theta_{c90} = \theta_{c90} - \theta_c \tag{45}$$

Now, the value of the table swivelling angle (θ_{c90}) will be corrected by ±180° or by ±360° as follows:

If $\Delta\theta_c < -7\pi/4$, then $\theta_c = \theta_{c90} + 2\pi$;
If $\Delta\theta_c \in [-\pi/4, -5\pi/4]$, then $\theta_c = \theta_{c90} + \pi$;
If $\Delta\theta_c \in [\pi/4, 5\pi/4]$, then $\theta_c = \theta_{c90} - \pi$;
If $\Delta\theta_c > 7\pi/4$, then $\theta_c = \theta_{c90} - 2\pi$;
Else $\theta_c = \theta_{c90}$;

Note: If $p_x^2 + p_y^2 < \delta_{yc}^2$ in Eq. 42, the discriminant of the argument of a function in this equation is smaller than zero. Therefore, its argument is not a real number. In this case, the solution does not exist for an angle θ_c that will lead the surface of machining to the machine X-axis. This is illustrated by an example shown in Fig. 9. For simplicity, it has been taken that the angular head axes intersect; a_3=0, and therefore p_x=X_5 and p_y=Y_5 hold. Here, we must machine the workpiece in the table centre or very close to it. However, the centre is displaced in relation to the X-axis, because of the thermal deflection, by the value δ_{yc}. If $X_5 = 0$ and $|Y_5| < |\delta_{yc}|$, no swivelling of the table can result in its centre being under the cutting tool. Therefore, this machining is impossible. The table base should be allowed to cool and the table axis should return to the zero position.

5.1.2 Worktable singular positions

The singular position of a rotary axis could provide two possible solutions to the inverse kinematics or the end positions of the axes. Sometimes, a rotary axis must make a quick turn, often ±180°, to produce the desired tool motion. The algorithm given in subsection 5.1.1 prevents the worktable from swivelling by ±180° or ±360° in a single interpolation period and extends the range of angle θ_c to [−360°+θ_{c90},360°+θ_{c90}].

Some possible singular positions of the worktable still remain and will be discussed now. Analysing Eq. 42, it is noticeable that in some specific situations, to correct for the motion caused by the thermal deflection δ_{yc}, the worktable swivels by ±180° or ±90° in short time intervals. These singular positions are presented below.

1. If p_x=0, then $\theta_c = \text{atan2}(-\sqrt{p_y^2 - \delta_{yc}^2}, -\delta_{yc})$. This means that, for the case when $P_y \to \delta_{yc}$ and $\delta_{yc} > 0$, it holds that $\theta_c \to 180°$, and for $\delta_{yc} < 0$, it holds that $\theta_c \to 0°$. If $P_y \le \delta_{yc}$, the discriminant, $D = p_y^2 - \delta_{yc}^2$, is smaller than or equal to zero; therefore, the assigned motion is not achievable.
2. If p_y=0, then $\theta_c = \text{atan2}(-\delta_{yc}, \sqrt{p_x^2 - \delta_{yc}^2})$. This means that for the case when $P_y \to \delta_{yc}$ and $\delta_{yc} > 0$, it holds that $\theta_c \to 90°$, and for $\delta_{yc} < 0$, it holds that $\theta_c \to 90°$. If $P_y \to \delta_{yc}$, the discriminant, $D = p_x^2 - \delta_{yc}^2$, is smaller than zero; therefore, the assigned motion is not achievable.
3. A special case of machining is when p_y=0 and δ_{yc}=0. Then, θ_c=atan2(0,p_x) holds; so, in changing the sign of the parameter p_x, the table swivels through an angle of ±180°. Table swivelling is performed here at a programmed velocity and a programmed acceleration while the remaining four axes do not move. The control algorithm itself provides for further continuation of motion along the X-axis in the positive direction.

5.2 Calculations of the angle θ_3

The angle θ_3, similar to angle C_t as described in subsection 4.1.2, can be calculated in a number of ways. If the

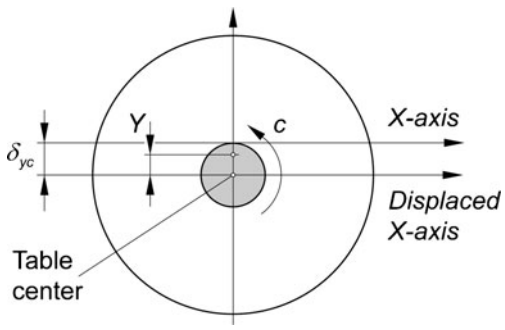

Fig. 9 Example of the displaced table centre when X_5=0 and $|Y_5|$<−δ_{yc} |

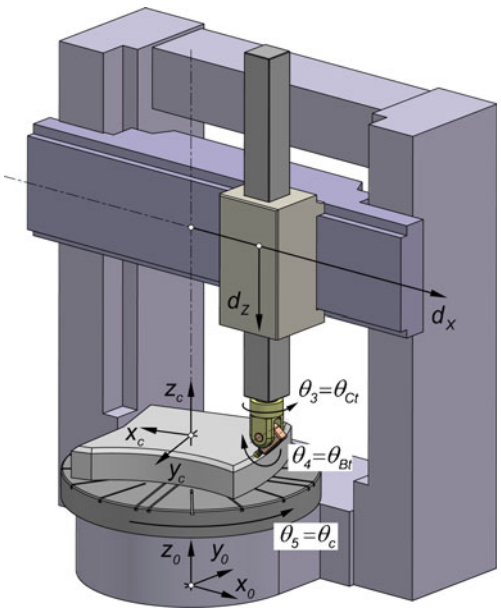

Fig. 10 Simulation model of the vertical five-axis turning centre

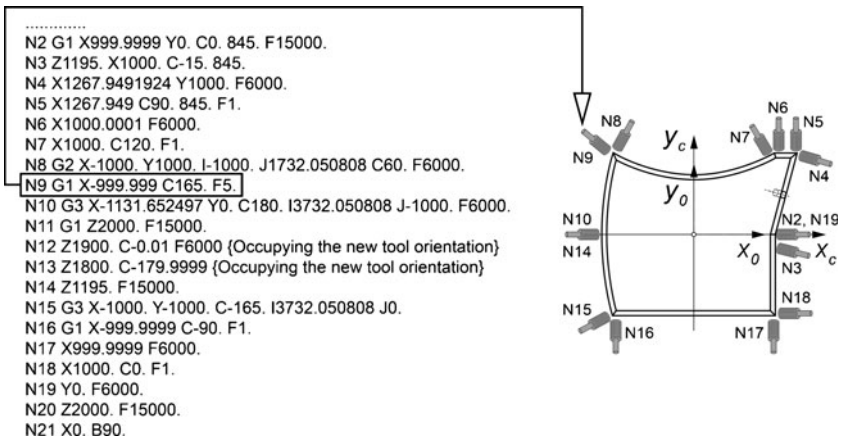

Fig. 11 The machining programme text and a schematic presentation of the programmed tool motion path in examples 1 and 2

programming is done in G code, and if the tool orientation is assigned by angles B_t and C_t, using Eq. 9, we can calculate the tool orientation matrix coefficients. Afterward, using terms (1,2) and (2,2) of Eq. 30, we can calculate angle θ_3 using the equation:

$$\theta_3 = \text{atan2}(c_c o_{x5} - s_c o_{y5}, -s_c o_{x5} - c_c o_{y5}) \tag{46}$$

In Section 4.1.2, it has been shown that components o_{x5} and o_{y5} do not depend on angle B_t and that they always lie in the x_0y_0 plane and are never simultaneously equal to 0. Hence, Eq. 46 can be used to calculate angle θ_3. When the table swivelling angle θ_c equals 0, Eq. 20, which is used to calculate the angle C_t, is identical to Eq. 46, which now reads: $\theta_3 = \text{atan2}(o_{x5}, -o_{y5})$.

As mentioned in Section 3, when a CAM system is used in programming, its output is the assigned tool position and the direction vector **a** given in the CL data file. This means that to determine the machine axis position, all nine tool-

Table 2 Machine components' positions and workpiece dimensions at the end of each movement segment when there is thermal error compensation for the machine base deflection in example 1

Line	$d_1=d_x$ [mm]	$d_2=d_z$ [mm]	θ_3 [°]	θ_4 [°]	θ_c [°]	X [mm]	Y [mm]	Z [mm]	B_t [°]	C_t [°]
	Inner coordinates obtained by inverse kinematics with compensation of the thermal base deflection					Workpiece dimensions obtained by forward kinematics (base thermal deflection is included)				
Initial point	215.0999	−255.0000	0.000016	90	0.000016	0.0000	0.0000	2,000	90	0.0000
N2	1,114.0517	−498.9518	0.010287	45	0.010287	999.9999	0.0000	2,000	45	0.0000
N3	1,110.5607	306.0482	−13.467774	45	1.532226	1,000.0000	0.0000	1,195	45	−15.0000
N4	1,685.5727	306.0482	−50.149372	45	−35.149372	1267.9492	1000.0000	1195	45	−15.0000
N5	1,687.8747	306.0482	48.705988	45	−41.294012	1,267.9490	1,000.0000	1,195	45	90.0000
N6	1,497.0599	306.0482	41.922135	45	−48.077865	1,000.0001	1,000.0000	1,195	45	90.0000
N7	1,447.9962	306.0482	70.648085	45	−49.351915	1,000.0000	1,000.0000	1,195	45	120.0000
N8	1,447.9962	306.0482	−70.632256	45	−130.632256	−1,000.0000	1,000.0000	1,195	45	60.0000
N9	1,514.0705	306.0482	27.850849	45	−137.149151	−999.9990	1,000.0000	1,195	45	165.0000
N10	1,245.7043	306.0482	0.009200	45	−179.990800	−1131.6525	0.0000	1,195	45	180.0000
N11	1,245.7043	−498.9518	0.009200	45	−179.990800	−1,131.6525	0.0000	2,000	45	180.0000
N12	1,017.8006	−398.9518	−179.999860	45	−179.989860	−1,131.6525	0.0000	1,900	45	−0.0100
N13	1,245.7043	−298.9518	0.009201	45	−179.990809	−1,131.6525	0.0000	1,800	45	−179.9999
N14	1,245.7043	306.0481	0.009201	45	−179.990809	−1,131.6525	0.0000	1,195	45	−179.9999
N15	1,514.0712	306.0481	−27.835685	45	−222.835685	1,000.0000	−1,000.0000	1,195	45	−165.0000
N16	1,497.0597	306.0481	41.922129	45	−228.077871	−999.9999	−1,000.0000	1,195	45	−90.0000
N17	1,497.0597	306.0481	−41.906819	45	−311.906819	999.9999	−1000.0000	1,195	45	−90.0000
N18	1,497.0598	306.0481	41.922132	45	−318.077868	1,000.0000	−1,000.0000	1,195	45	0.0000
N19	1,114.0518	306.0481	0.010287	45	−359.989713	1,000.0000	0.0000	1,195	45	0.0000
N20	1,114.0518	306.0481	0.010287	45	−359.989713	1,000.0000	0.0000	2,000	45	0.0000
N21	215.0999	−255.0000	0.053298	90	−359.946702	0.0000	0.0000	2,000	90	0.0000

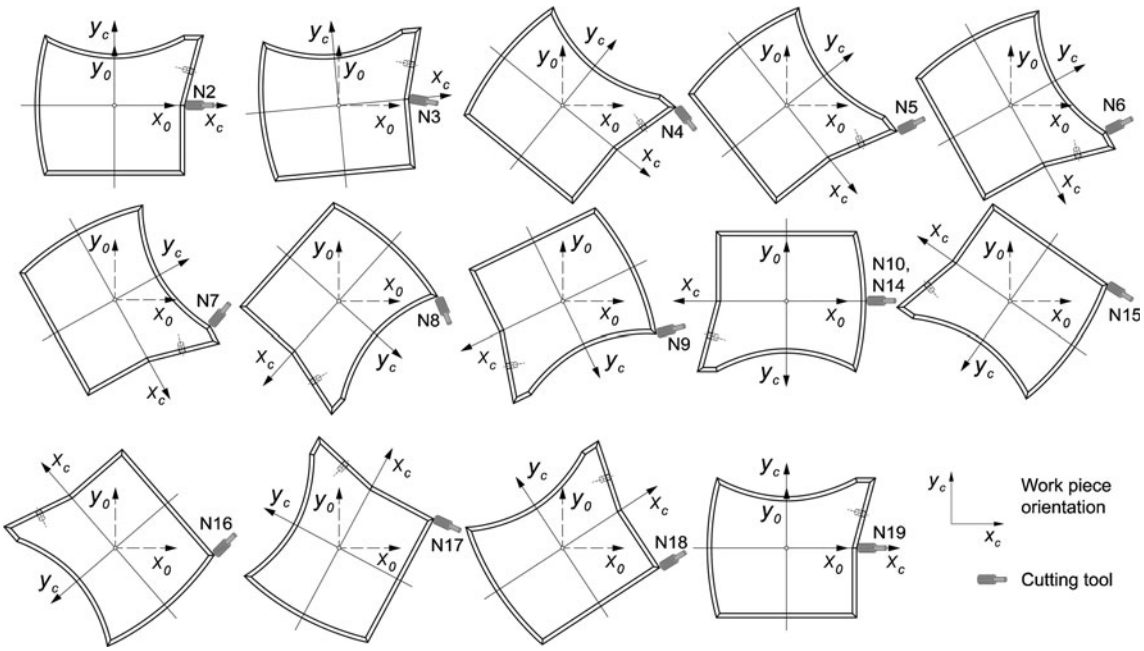

Fig. 12 Schematic presentation of the workpiece orientations and the tool positions and orientations at the end of machining given in the line N2-N10 and N14-N19 of the NC programme in example 1

orientation matrix terms cannot be used: only components a_{x5}, a_{y5} and a_{z5} are of use. Term (3,3) of Eq. 31 yields:

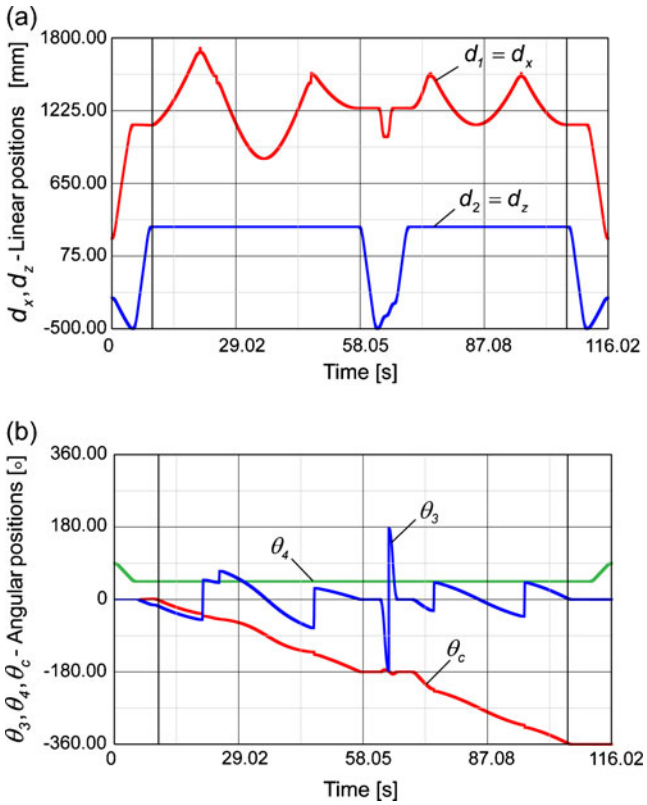

Fig. 13 Diagrams of **a** how the translational inner coordinates $d_1=d_x$ and $d_2=d_z$ are changing and **b** how the rotational inner coordinates θ_3, θ_4 and θ_c are changing in example 1

$$\theta_3 = \text{atan2}(s_c a_{x5} + c_c a_{y5}, c_c a_{x5} - s_c a_{y5}) \tag{47}$$

and

$$\theta_3 = \text{atan2}(-s_c a_{x5} - c_c a_{y5}, -c_c a_{x5} + s_c a_{y5}) \tag{48}$$

The previous two equations, for the case when the work table swivelling angle θ_c equals zero, are identical to Eqs. 24 and 25. As mentioned in Section 4.1.2, the values of these two solutions differ by 180°. For B_t=0°, components a_{x5} and a_{y5} equal 0, so Eqs. 47 and 48 always yield θ_3=0° or θ_3= 180°, irrespective of the current value of angle θ_3. We now will present the algorithm that, in the application of either of the two previous equations, will prevent abrupt angular head swivelling around the vertical axis and will yield a solution for angle θ_3 when B_t=0°. Here, θ_{3prev} denotes the angle θ_3 in the previous interpolation period.

If $\theta_3 - \theta_{3prev} \in [\pi/2, 3\pi/2]$, then $\theta_3 = \theta_3 - \pi$;
If $\theta_3 - \theta_{3prev} \in [-\pi/2, -3\pi/2]$, then $\theta_3 = \theta_3 + \pi$;
If $a_{x5} = 0$ and $a_{y5} = 0$, then $\theta_3 = \theta_{3prev}$;

5.3 Calculations of the angle θ_4

When programming is performed in a CAM system using the CL data file, the angle θ_4 can be calculated using terms (1,2) and (2,2) of Eq. 31 such that:

$$\theta_4 = \text{atan2}(c_3(s_c a_{y5} - c_c a_{x5}) - s_3(s_c a_{x5} + c_c a_{y5}), -a_{z5}) \tag{49}$$

In the case that the tool orientation is given by angles B_t and C_t, angle θ_4 can be calculated in other ways using

Table 3 Machine components' positions and workpiece dimensions at the end of each movement segment when there is no thermal error compensation of the machine base deflection in example 2

Line	$d_1=d_x$ [mm]	$d_2=d_z$ [mm]	θ_3 [°]	θ_4 [°]	θ_c [°]	X [mm]	Y [mm]	Z [mm]	B_t [°]	C_t [°]
	Inner coordinates obtained by inverse kinematics without compensation of the thermal base deflection					Workpiece dimensions obtained by forward kinematics (base thermal deflection is included)				
Initial point	215.0000	−255.0000	0.000000	90	0.000000	−0.1000	0.2000	2,000	90	0.0000
N2	1,113.9517	−498.9518	0.000000	45	0.000000	999.8999	0.2000	2,000	45	0.0000
N3	1,110.4607	306.0482	−13.478093	45	1.521907	999.9053	0.2026	1,195	45	−15.0000
N4	1,685.4727	306.0482	−50.156171	45	−35.156171	1,267.7523	1,000.1059	1,195	45	−15.0000
N5	1,687.7747	306.0482	48.699199	45	−41.300801	1,267.7419	1,000.0842	1,195	45	90.0000
N6	1,496.9599	306.0482	41.914480	45	−48.085520	999.7845	1,000.0592	1,195	45	90.0000
N7	1,447.8963	306.0482	70.640171	45	−49.359829	999.7831	1,000.0543	1,195	45	120.0000
N8	1,447.8963	306.0482	−70.640171	45	−130.640171	−1,000.0866	999.7939	1,195	45	60.0000
N9	1,513.9705	306.0482	27.843280	45	−137.156720	−1,000.0617	999.7853	1,195	45	165.0000
N10	1,245.6043	306.0482	0.000000	45	−180.000000	−1131.5525	−0.2000	1,195	45	180.0000
N11	1,245.6043	−498.9518	0.000000	45	−180.000000	−1,131.5525	−0.2000	2,000	45	180.0000
N12	1,017.7007	−398.9518	179.9889	45	−180.001120	−1,131.5525	−0.2000	1,900	45	−0.0100
N13	1,245.6043	−298.9518	0.000091	45	−180.000009	−1,131.5525	−0.2000	1,800	45	−179.9999
N14	1,245.6043	306.0482	0.000091	45	−180.000009	−1,131.5525	−0.2000	1,195	45	−179.9999
N15	1,513.9712	306.0482	−27.843254	45	−222.843254	−999.7907	−1,000.0786	1,195	45	−165.0000
N16	1,496.9597	306.0482	41.914474	45	−228.085526	−999.7843	−1,000.0592	1,195	45	−90.0000
N17	1,496.9598	306.0482	−41.914474	45	−311.914474	1,000.0819	−999.7920	1,195	45	−90.0000
N18	1,496.9598	306.0482	41.914477	45	−318.085523	1,000.0592	−999.7843	1,195	45	0.0000
N19	1,113.9518	306.0482	0.000000	45	−360.000000	999.9000	0.2000	1,195	45	0.0000
N20	1,113.9518	−498.9518	0.000000	45	−360.000000	999.9000	0.2000	2,000	45	0.0000
N21	−215.0000	−255.0000	0.000000	90	−360.000000	−0.1000	0.2000	2,000	90	0.0000

different terms of Eqs. 30 and 31, e.g.

$$\theta_4 = \text{atan2}(-n_{z5}, -a_{z5}) \tag{50}$$

5.4 Calculations of the parameters, d_1 and d_2

Terms (1,4) and (3,4) of Eq. 30 that determine the motion along the X and Z axis yield:

$$d_1 = d_x = c_c X_5 - s_c Y_5 - c_3 a_3 + \delta_{xc} \tag{51}$$

$$d_2 = d_z = d_{zc} - Z_5 \tag{52}$$

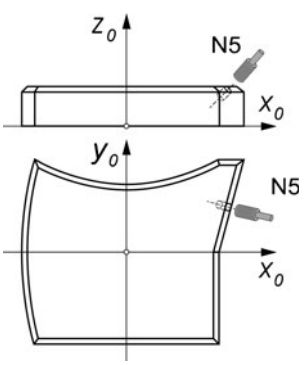

Fig. 14 Schematic presentation of the programmed tool motion path in example 3

5.5 Mathematical explanation of the machining error caused by the base thermal deflection

Equations 6 and 7 show that the base thermal deflection causes the error of the workpiece dimensions X and Y, given by the following equations:

$$\Delta X = -c_c \delta_{xc} - s_c \delta_{yc} \text{ and} \tag{53}$$

$$\Delta Y = s_c \delta_{xc} - c_c \delta_{yc} \tag{54}$$

During the machining, due to the cooling of the worktable bearing, the values of δ_{xc} and δ_{yc} are changing. That additionally changes the dimensions and the geometry of the workpiece. The proposed algorithm changes the table swivelling and the ram cross-section translation, Eqs. 42 and 51, in order to eliminate this error.

6 Results verification for the proposed control algorithm

The solution for the forward and the inverse kinematics, which makes the proposed control algorithm, was tested on the off-line programming system of the controller

Table 4 Successive machine components' positions and tool locations during drilling in example 3

	$d_1=d_x$ [mm]	$d_2=d_z$ [mm]	θ_3 [°]	θ_4 [°]	θ_c [°]	X [mm]	Y [mm]	Z [mm]	B_t [°]	C_t [°]
	Inner coordinates obtained by inverse kinematics with compensation of the thermal base deflection					Workpiece dimensions obtained by forward kinematics (base thermal deflection is included)				
Initial point	1,330.1451	306.0482	−35.708406	45	−20.708406	1,133.9740	500.0000	1,195.0000	45	−15
Successive machine components' positions and tool locations	1,303.3383	339.2425	−36.560207	45	−21.560207	1,101.9107	508.5913	1,161.8057	45	−15
	–	–	–	–	–	–	–	–	–	–
	1,274.5290	375.3392	−37.526924	45	−22.526924	1,067.0439	517.9337	1,125.7089	45	−15
	–	–	–	–	–	–	–	–	–	–
	1,246.0994	411.4360	−38.538058	45	−23.538058	1,032.1771	527.2763	1,089.6122	45	−15
	–	–	–	–	–	–	–	–	–	–
	1,220.2227	444.7482	−39.512721	45	−24.512721	1,000.0000	535.8980	1,056.3000	45	−15

developed at the Lola Institute. This controller was obtained by extending the Lola-Industrial Robot Language [21] with the commands for a machine tool by integrating the new solutions for the forward and inverse kinematics of a vertical five-axis turning centre in it and by adapting its trajectory planner to novel tool motion commands.

Here, three examples of the machining are displayed, illustrating the efficiency of the proposed control algorithm. It has been shown that this algorithm fully accomplishes the assigned machine motion during milling, drilling and boring. It has also been shown that the base thermal deflection, if there is no compensation for the machine motion, causes inaccuracy in the machining.

Figure 10 shows a model of the machine in which the example simulations of the machining were performed. It also shows the inner coordinates, d_1, d_2, θ_3, θ_4 and θ_c, of the machine.

Programmes identical to that of the five-axis gantry milling machine were written. Three examples of machining were created. In all the examples, because of the base thermal deflection (Figs. 2 and 4), the rotating table centre was displaced by δ_{xc}=0.1 mm and δ_{yc}=−0.2 mm. In examples 1 and 3, the thermal compensation was performed, and example 2 was performed without it.

In examples 1 and 2, the machine carried out five-axis milling. The machining programme text and the programmed tool motion path in these two examples are presented in Fig. 11.

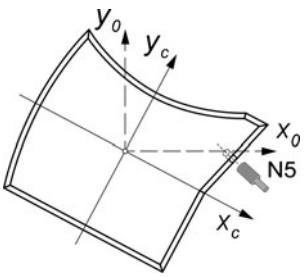

Fig. 15 The workpiece orientation and tool location during drilling or boring in example 3

Example 1 The positions of the machine components and the tool locations (workpiece dimensions) at the end of each movement segment in example 1 are given in Table 2. If we compare the machining programme text from Fig. 11 with the values of X, Y, Z, B_t and C_t from Table 2, we will see that the proposed control algorithm entirely achieves the tool's assigned motion. Also, it fully compensates for the base thermal deflection. Therefore, it is possible to obtain an accurate workpiece, even if thermal deflection occurs.

Figure 12 schematically displays the workpiece orientations (coordinates x_c and y_c) and the tool positions and orientations at the end of each movement segment of machining given in the lines N2-N10 and N14-N19 of the NC programme in example 1 (Fig. 11). Illustrated here is the way in which two translational and three rotary axes for five-axis milling achieve the motion achieved by three translational and two rotary axes.

Figures 13a, b display diagrams of how the inner coordinates d_1, d_2, θ_3, θ_4 and θ_c are changing in example 1. These diagrams show that the proposed control algorithm carries out five-axis milling without abrupt movements of the machine links. Figure 13b shows abrupt swivelling of θ_3 on the beginning of the movement N 13 (Fig. 11) from −179.999860° to 179.995111°. This abrupt swivelling happens outside the machining zone. It disables swivelling of θ_3 outside of allowed angle range of ±180°. Abrupt swivelling is possible to avoid by using the programmed movement of θ_3 while the remaining four axes do not move. But this movement could be performed by another algorithm, which is not presented in this paper (point-to-point movement).

Example 2 Table 3 shows the results from example 2. The positions of the machine components obtained by inverse kinematics without compensation of the thermal base

deflection and the workpiece dimensions obtained by forward kinematics, where the base thermal deflection is included at the end of each movement segment are given. It is noticeable that thermal deflection of the machine base causes errors in the tool movement and inaccuracy of the workpiece.

By comparing the values in the columns for X and Y in the Table 3, where there is no thermal error compensation of the machine base deflection, with the same columns in the Table 2, where there is this thermal error compensation, we could see that the proposed algorithm fully eliminates the inaccuracy of machining caused by the thermal deflection of the base.

Example 3 In example 3, the machine executes the drilling out of the table centre in directions not parallel with the machine basic coordinate axes $x_0y_0z_0$ (Fig. 4). The programmed tool motion path in this example is presented in Fig. 14. The machining programme command for the movement in this example reads: N5 X1000. Y535.898 Z1056.3C-15. B45. F500.

The successive positions of the machine components and the tool locations (workpiece dimensions) during motion in example 3 are given in Table 4. It is evident that the proposed control algorithm entirely realises the tool assigned motion during the drilling at an arbitrary position and angle. Also, it fully compensates for the base thermal deflection. Figure 15 schematically displays the workpiece orientation and the tool location during drilling in example 3.

7 Conclusion

It has been shown that on a five-axis turning centre with two translational and three rotational axes, in addition to the turning, it is possible to achieve five-axis milling, drilling and boring identical to that of a milling machine with three translational and two rotational axes. A control algorithm to achieve this was presented. Using this algorithm, machine programming is possible in the same way that it is done for a five-axis milling machine, which essentially simplifies writing the machining programme or taking over the CL data file from CAM systems developed for the milling machines.

Forward and inverse kinematics, based on the D–H formulation, have been solved for the case of utilising the two-axis angular head with non-intersecting axes. This increases the achievability of machining and allows for certain machining without the machine taking any singular positions. The control algorithm for the angular head with intersecting axes is simplified. Also, this algorithm extends the table swivelling angle range to approximately ±360°. Thus, additional positioning of the worktable and the angular head during machining is decreased.

The proposed algorithm fully eliminates the inaccuracy of machining caused by the thermal deflection of the base.

The proposed control method is much more complex then the algorithms which are in use today, but it increases the machining possibility and accuracy. The today's solutions for θ_c and d_1 are for the case when the angular head axes intersect and when there is no thermal deflection. They read: $\theta_c = \text{atan2}(-Y_5, X_5)$ and $d_1 = d_x = c_c X_5 - s_c Y_5$.

Acknowledgments This research is supported by the Ministry of Science and Technological Development of Serbia under the project Research and Development of the New Generation of Vertical Five-Axis Turning Centre (2008–2010), no. 14026.

References

1. López de Lacalle LN, Lamikiz A (2008) Machine tools for high performance machining. Springer Verlag, ISBN: 978-1-84800-379-8
2. Mahbubur RMD, Heikkala J, Lappalainen K, Karjalainen JA (1997) Positioning accuracy improvement in five-axis milling by post processing. Int J Mach Tools Manuf 37(2):223–236
3. Lamikiz A, López de Lacalle LN, Ocerin O, Díez D, Maidagan E (2008) The Denavit and Hartenberg approach applied to evaluate the consequences in the tool tip position of geometrical errors in five-axis milling centres. Int J Adv Manuf Technol 37:122–139
4. Liu H, Li B, Wang X, Tan G (2011) Characteristics of and measurement methods for geometric errors in CNC machine tools. Int J Adv Manuf Technol 54:195–201
5. Yang SH, Kim CK-H, Park ĆY-K, Lee ĆS-G (2004) Error analysis and compensation for the volumetric errors of a vertical machining centre using a hemispherical helix ball bar test. Int J Adv Manuf Technol 23:495–500
6. Elbestawit MA, Srivasta AK, Veldhuis SC (1995) Modelling geometric and thermal errors in a five-axis CNC machine tool. Int J Mach Tools Manuf 35(9):1321–1337
7. Lin Y, Shen Y (2003) Modelling of five-axis machine tool metrology models using the matrix summation approach. Int J Adv Manuf Technol 21(4):243–248
8. Nawara L, Kowalski J, Sladek J (1989) The influence of kinematic errors on the profile shapes by means of CMM. CIRP Ann 38(1):511–516
9. Tseng P-C, J-Ho H (2002) A study of high-precision CNC lathe thermal errors and compensation. Int J Adv Manuf Technol 19:850–858
10. Zhang H, Yang J, Zhang Y, Shen J, Wang C (2011) Measurement and compensation for volumetric positioning errors of CNC machine tools considering thermal effect. Int J Adv Manuf Technol 55:275–283
11. Ramesh R, Mannan MA, Poo AN (2002) Support vector machines model for classification of thermal error in machine tools. Int J Adv Manuf Technol 20:114–120
12. Pahk HJ, Lee SW (2002) Thermal error measurement and real time compensation system for the CNC machine tools incorpo-

rating the spindle thermal error and the feed axis thermal error. Int J Adv Manuf Technol 20:487–494
13. López de Lacalle LN, Lamikiz A, Sánchez JA, Salgado MA (2007) Toolpath selection based on the minimum deflection cutting forces in the programming of complex surfaces milling. Int J Mach Tools Manuf 47:388–400
14. López de Lacalle LN, Lamikiz A, Sánchez JA, Salgado MA (2004) Effects of tool deflection in the high-speed milling of inclined surfaces. Int J Adv Manuf Technol 24(9–10):621–631
15. Lee RS, She CH (1997) Developing a postprocessor for three types of five-axis machine tools. Int J Adv Manuf Technol 13 (9):658–665
16. Sørby K (2007) Inverse kinematics of five-axis machines near singular configurations. Int J Mach Tools Manuf 47:299–306
17. Bohez ELJ (2002) Five-axis milling machine tool kinematic chain design and analysis. Int J Mach Tools Manuf 42:505–520
18. Lee RS, Lin YH (2010) Development of universal environment for constructing 5-axis virtual machine tool based on modified D–H notation and open GL. Robot Comput-Integrated Manuf 26:253–262
19. Paul RP (1984) Robot manipulators: mathematics, programming and control. The MIT Press, Cambridge
20. López de Lacalle LN, Lamikiz A, Muñoa J, Sánchez JA (2005) The CAM as the centre of gravity of the five-axis high speed milling of complex parts. Int J Prod Res 43(10):1983–1999
21. Pavlović M, Kvrgić V, Velašević D (1994) L-IRL: high level programming language for robots. In Proc of the European Robotics and Intelligent Systems Conference, Malaga, Spain